Gait Recognition Based on Tensor Analysis of Acceleration Data from Wearable Sensors

Kshitij Bichave, Owen Brewer, Max Gusinov, Panos P. Markopoulos, and Ivan Puchades†
Dept. of Electrical and Microelectronic Engineering, Rochester Institute of Technology, Rochester, NY 14623
E-mail: {kvb3025, ojb3782, mxg8923, panos, ivan.puchades}@rit.edu

***Abstract*—We use commercial wearable sensors to collect three-dimensional acceleration signals from various gaits. Then, we organize the collected measurements in three-way tensors and present a simple, efficient gait classification scheme based on TUCKER2 tensor decomposition. The proposed scheme derives as multi-linear generalization of the nearest-subspace classifier. Our experimental studies show that the proposed approach manages to automatically identify the motion axes of interest and classify walking, jogging, and running gaits with high accuracy.**

***Index Terms*—Acceleration, gait recognition, IMU, MEMS, tensor decomposition, wearable sensors.**

I. Introduction

Gait recognition/classification has attracted extended research interest over the past decade. Modern applications of gait analysis include, but are not limited to, security (e.g., biometric identification) [1], [2], sports medicine and injury rehabilitation [3], [4], and disease diagnosis/prognosis [5]–[9].

Popular sensing modalities for gait recognition include radar, imaging/video, and acceleration. In [10], authors used radar micro-Doppler signatures to analyze gaits of elderly. More recently, in [11] and [12], radar measurements were used for gait abnormality classification and gait-cycle estimation, respectively. A detailed presentation of methods and applications for radar-based gait recognition is offered in [13]. Authors in [14] presented a method for multi-view video-based gait recognition; a thorough review of vision-based gait recognition is offered in [15]. Another promising sensing modality for gait analysis is acceleration. The research background on acceleration-based gait recognition is presented in [16], [17]. Detailed assessment of acceleration signals is offered in [18]–[20]. Other modalities that have been recently used for gait recognition include foot/floor pressure [21], Wi-Fi signals [22], as well as various measurements from Microsoft Kinect [23], [24], smartwatches [25], and smartphones [26], [27].

At the same time, the use of wearable sensors has been continuously increasing over the past years in an array of mainstream applications related to fitness and health-condition monitoring [7]. A variety of available wearable sensing devices, comprising sensors and respective signal processing algorithms, are now employed to measure and analyze diverse activities ranging from simple step counting to fatigue detection and injury prevention for professional athletes [28], [29].

†Corresponding author.

This work was supported in part by the RIT Kate Gleason College of Engineering, under a FEAD grant, the RIT Honors Program, and the U.S. National Science Foundation, under grant OAC-1808582.

Regretfully, the sensing capabilities of such devices are often under-utilized due to the complexity associated with storing, transferring, processing, and, more importantly, interpreting the large amounts of collected data. Instead, information-bearing variance is often eliminated by either averaging (e.g., average distance walked per day), or isolation of extrema (min/max) [30]. For example, beyond mere step counting, continuous measurements of leg-motion acceleration have clearly demonstrated the capacity to provide very important insights on the wellness of patients [9], [31].

The increasing popularity of wearables can be in part attributed to their high sensing accuracy, enabled by significant advances in microelectromechanical systems (MEMS) technology [32] –and specifically inertial sensors (accelerometers, gyroscopes), commonly combined in inertial measurement units (IMU) [33]–[35]. MEMS-IMUs are low-cost/low-power, small, lightweight, portable, and unobtrusive. Furthermore, inertial signals can allow for complex motion analysis [36].

In this work, we focus on gait classification based on acceleration signals collected from low-cost commercial wearable IMUs. Specifically, we collect acceleration data across three dimensions, for walking, jogging, and running. Then, we organize the collected data in three-way tensors, and process them as such, so that measurement dependencies across the time and sensing-orientation dimensions are preserved and leveraged towards improved gait recognition. Finally, we employ a simple and efficient scheme for gait classification based on TUCKER2 tensor decomposition [37]. Our experimental studies show that the proposed approach manages to classify different gaits with very high accuracy.

II. Experimental Methods

A. Data Acquisition

For data acquisition, we used the MetaMotionR Developer Kit of MBIENTLAB Inc. [38] which combines the low-power IMU BMI160 [39], manufactured by BOSCH, together with a pressure sensor, a magnetometer, a generic temperature sensor, an ambient light sensor, and 8MB of flash memory. The kit is bluetooth enabled, powered by an 80mAH lithium ion 3.7V battery, and equipped with an ARM Cortex M4F processor. In this work, we only collected and processed acceleration data collected by the BMI160 IMU, which was set up to provide a sensitivity range of +/-16g at 2048LSB/g and a sample frequency of 200Hz.

The sensing kit was placed on the right shoe heel of three participants (3±1cm above the ground) as shown in Fig. 1.

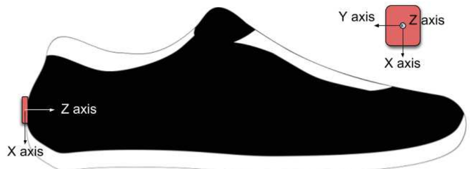

Fig. 1: Sensor placement and axis orientation.

Fig. 1 also shows the orientation of the three acceleration axes across which measurements were collected. Each participant wore shoes with different heel width and material depending on individual comfort. The participants were between 18 and 24 years of age, with weight in the range 100-200lb and no injury or pain. All measurements were collected over the same day, indoors, while the participants were walking, jogging, and running on a 100-feet-long straight track.

B. Data Pre-processing and Tensor Formation

With the process described above, we collected a varying-length real-valued signal for each subject, gait, and acceleration axis. Each of these signals comprises a sequence of successive gait cycles. For the sake of clarity, we henceforth assign indices $p = 1, 2, 3$ to the three participants, $g = 1, 2, 3$ to gaits walking, jogging, and running, respectively, and $a = 1, 2, 3$ to axes X, Y, and Z (see Fig. 1), respectively. Accordingly, we denote by $\{x_{p,g,a}[n]\}$ the length-$N_{p,g}$ acceleration signal for participant p, gait g, and axis a. $N_{p,g}$ depends on the sampling rate and measurement duration and varies across each participant and gait. In the sequel, we present how these signals were processed, before they were used for gait learning and recognition.

Jitter Smoothing: First, we apply to each of the collected acceleration signals a moving average filter (MAF) that smooths short-term jitters, while it keeps the long term pattern practically intact. Specifically, the output of the MAF when applied to acceleration signal $x_{p,g,a}[n]$ is given by

$$\tilde{x}_{p,g,a}[m] = \frac{1}{\mathrm{dur}(m)} \sum_{n=\mathrm{low}(m)}^{\mathrm{upp}(m)} x_{p,g,a}[n], \tag{1}$$

for $m = 1, 2, \ldots, N_{p,g}$, where $\mathrm{upp}(m) = \min\{N_{p,g}, m + \lfloor B/2 \rfloor\}$, $\mathrm{low}(m) = \max\{1, m - \lfloor B/2 \rfloor\}$, $\mathrm{dur} = \mathrm{upp}(m) - \mathrm{low}(m) + 1$, and odd smoothing window size B.

Data Segmentation and Length Normalization: The smoothed acceleration signal $\{\tilde{x}_{p,g,a}[n]\}$ corresponds to multiple successive gait cycles. In the next pre-processing step, we segment successive cycles, jointly across all axes (i.e., same segmentation for $\tilde{x}_{p,g,1}[n]$, $\tilde{x}_{p,g,2}[n]$, and $\tilde{x}_{p,g,3}[n]$). First, we identify successive heel-offs by the deepest local minima of the Z-axis signal; then, for each heel-off, we identify the previous zero-crossing as the start point of the respective gait cycle and segment $\{\tilde{x}_{p,g,a}[n]\}$ at these points (other methods for gait-event detection in acceleration signals were presented in [20], [40], [41]). Thus, for each gait cycle in $\{\tilde{x}_{p,g,a}[n]\}$, we obtain a sequence of short discrete-time signals of varying length (across p and g). Finally, we normalize by interpolation or sub-sampling the length of all single-cycle signals to some value L, determined by the average cycle duration and the sampling rate. The length-L signals obtained with the above procedure are henceforth referred to as the *acceleration signatures*. Fig. 2 illustrates the signal smoothing, segmentation, and length-normalization for walking.

Data Organization in Tensors: Each length-L acceleration signature can also be represented as a vector in $\mathbb{R}^L$. Let $\mathbf{x}_{p,g,a,c} \in \mathbb{R}^L$ be the signature for participant p, gait g, axis a, and cycle index c. Henceforth, we fix the same number of C cycles per (p, g, a) (C derives by the minimum value of $N_{p,g}/L$ across p and g). Concatenating the signatures $\mathbf{X}_{p,g,c} = [\mathbf{x}_{p,g,1,c}, \mathbf{x}_{p,g,2,c}, \mathbf{x}_{p,g,3,c}]^\top \in \mathbb{R}^{3 \times L}$, we form a 2D (i.e., matrix) participant-gait acceleration signature. Finally, for all combinations of p and c (in arbitrary order), we concatenate $\mathbf{X}_{p,g,c}$ as frontal slabs of the gait tensor dataset $\underline{\mathbf{X}}_g \in \mathbb{R}^{3 \times L \times N}$, for $N = 3C$.

III. Tensor Decomposition for Learning and Classification

In this paper, we present a simple tensor-based method for the classification of 2D gait signatures. The presented classification method is based on TUCKER2 [37], [42], [43] tensor decomposition and derives as a multi-linear generalization of the standard nearest-subspace classifier (NSC) [44]. Tensor methods have also been successfully used in the past for gait recognition from different sensing modalities [45]–[49].

We consider that $N_{\mathrm{tr},g}$ training 2D signatures are available from gait g (frontal slabs of tensor $\underline{\mathbf{X}}_g$) and organize them in the training tensor $\underline{\mathbf{X}}_{\mathrm{tr},g} \in \mathbb{R}^{3 \times L \times N_{\mathrm{tr},g}}$. For simplicity, we denote by $\mathbf{X}_{\mathrm{tr},g}(n)$ the n-th frontal slab of $\underline{\mathbf{X}}_{\mathrm{tr},g}$, $[\underline{\mathbf{X}}_{\mathrm{tr},g}]_{:,:,n}$. The proposed classifier seeks the pair of orthonormal bases ($\mathbf{U}_g \in \mathbb{R}^{3 \times d_{\mathrm{axis}}}, \mathbf{V}_g \in \mathbb{R}^{L \times d_{\mathrm{time}}}$), for $d_{\mathrm{axis}} \in \{1, 2, 3\}$ and $d_{\mathrm{time}} \in \{1, 2, \ldots, L\}$, that maximizes the aggregate low-rank projection of the signatures of gait g. That is, we wish to solve

$$(\mathbf{U}_g, \mathbf{V}_g) = \underset{\substack{\mathbf{U} \in \mathbb{R}^{3 \times d_{\mathrm{axis}}};\, \mathbf{U}^\top \mathbf{U} = \mathbf{I}_{d_{\mathrm{axis}}} \\ \mathbf{V} \in \mathbb{R}^{L \times d_{\mathrm{time}}};\, \mathbf{V}^\top \mathbf{U} = \mathbf{I}_{d_{\mathrm{time}}}}}{\operatorname{argmax}} \sum_{n=1}^{N_{\mathrm{tr},g}} \left\| \mathbf{U}^\top \mathbf{X}_{\mathrm{tr},g}(n) \mathbf{V} \right\|_F^2, \tag{2}$$

where the squared Frobenius norm $\| \cdot \|_F^2$ returns the sum of the squared entries of its matrix argument. The problem formulation in (2) is also known as Generalized Low-Rank Approximation of Matrices (GLRAM) [50], [51], 2D-PCA [37], Multilinear-PCA (MPCA) [46], or TUCKER2 [42] decomposition of the training tensor $\underline{\mathbf{X}}_{\mathrm{tr},g} \in \mathbb{R}^{3 \times L \times N_{\mathrm{tr},g}}$. The notion behind this formulation is that $(\mathbf{U}_g, \mathbf{V}_g)$ provide a subspace description for the 2D-data of gait g, reducing their dimensionality and suppressing any low-variance noise components in the measurements. In this work, we consider $d_{\mathrm{axis}} = 1$, so that $\mathbf{U}_g = \mathbf{u}_g \in \mathbb{R}^3$ is a vector that optimally combines measurements across the three axes, in a way that maximizes the preservation of variance. Accordingly, matrix signature $\mathbf{X}_g(n) \in \mathbb{R}^{3 \times L}$ is reduced to the vector signature $\mathbf{y}_g^\top(n) = \mathbf{u}_g^\top \mathbf{X}_g(n) \mathbf{V}_g \in \mathbb{R}^{1 \times d_{\mathrm{time}}}$. A schematic illustration of the presented TUCKER2 decomposition is offered in Fig. 3.

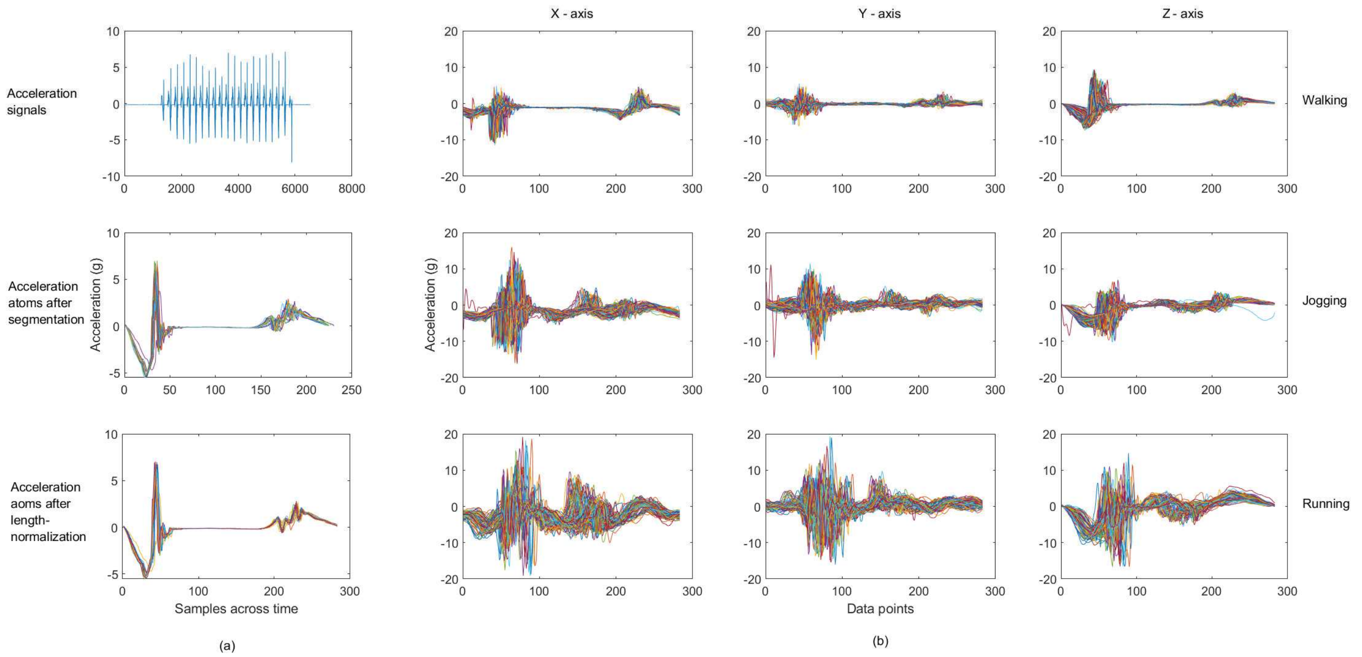

Fig. 2: (a) Acceleration measurements for walking. First row: Raw acceleration signal for Z-axis; Second row: Acceleration signatures after segmentation; Third row: Acceleration signatures after length normalization. (b) Acceleration measurements for walking, running, and jogging. First row: X-axis, Y-axis, Z-axis for walking; Second Row: X-axis, Y-axis, Z-axis for jogging; Third Row: X-axis, Y-axis, Z-axis for running.

Solution to TUCKER2 tensor decomposition in (2) is commonly pursued by means of the Higher-Order Singular-Value Decomposition (HOSVD) algorithm, or the Higher-Order Orthogonal Iterations (HOOI) [37], [50] algorithm. To achieve jointly optimal dimensionality reduction across the orientation-axes and time domains, in this work we employ HOOI – we recall that, instead, HOSVD would return $(\mathbf{U}_g, \mathbf{V}_g)$ by disjoint singular-value decompositions (SVD) of the mode-1 and mode-2 flattenings/unfoldings of $\underline{\mathbf{X}}_{\text{tr},g}$. Moreover, HOOI is known to attain higher value to the metric in (2) than HOSVD, which implies that it delivers bases that better preserve the original data variance. A brief description of the HOOI procedure follows.

First $\mathbf{u}_g$ is initialized to the dominant left-singular vector (SV) of $\mathbf{F}_{g,1} = [\mathbf{X}_{\text{tr},g}(1), \ldots, \mathbf{X}_{\text{tr},g}(N_{\text{tr},g})] \in \mathbb{R}^{3 \times L N_{\text{tr},g}}$, $\mathbf{u}_g^{(0)}$, obtainable by standard SVD. Then, $\mathbf{V}_g$ is initialized to the d_{time} dominant left-SVs of $\mathbf{F}_{g,2} = [\mathbf{X}_{\text{tr},g}(1)^\top, \ldots, \mathbf{X}_{\text{tr},g}(N_{\text{tr},g})^\top] \in \mathbb{R}^{L \times 3 N_{\text{tr},g}}$. Subsequently, the algorithm proceeds iteratively. At the t-th iteration step, the bases are updated as

$$\mathbf{u}_g^{(t)} = \underset{\mathbf{u} \in \mathbb{R}^3; \|\mathbf{u}\|_2 = 1}{\text{argmax}} \sum_{n=1}^{N_{\text{tr},g}} \|\mathbf{u}^\top \mathbf{X}_{\text{tr},g}(n) \mathbf{V}_g^{(t-1)}\|_F^2 \tag{3}$$

and

$$\mathbf{V}_g^{(t)} = \underset{\mathbf{V} \in \mathbb{R}^{L \times d_{\text{time}}}; \mathbf{V}^\top \mathbf{V} = \mathbf{I}_{d_{\text{time}}}}{\text{argmax}} \sum_{n=1}^{N_{\text{tr},g}} \|\mathbf{V}^\top \mathbf{X}_{\text{tr},g}(n)^\top \mathbf{u}_g^{(t)}\|_F^2. \tag{4}$$

The solution to (3) is given by the dominant left-SV of $[\mathbf{X}_{\text{tr},g}(1)\mathbf{V}_g^{(t-1)}, \ldots, \mathbf{X}_{\text{tr},g}(N_{\text{tr},g})\mathbf{V}_g^{(t-1)}] \in \mathbb{R}^{3 \times d_{\text{time}} N_{\text{tr},g}}$. The solution to (4) is given by the d_{time} dominant left-SVs of $[\mathbf{X}_{\text{tr},g}(1)^\top \mathbf{u}_g^{(t)}, \ldots, \mathbf{X}_{\text{tr},g}(N_{\text{tr},g})^\top \mathbf{u}_g^{(t)}] \in \mathbb{R}^{L \times N_{\text{tr},g}}$. Thus, overall, HOOI delivers an approximate (in general) solution to TUCKER2 in (3) by a sequence of matrix SVDs. It is worth noting that the HOOI iterations converge in the metric of (3). Upon convergence (or earlier termination), HOOI returns the gait class bases $(\mathbf{u}_g, \mathbf{V}_g)$ and the training process is completed.

When a new 2D signature $\mathbf{X} \in \mathbb{R}^{3 \times L}$ (from an unknown gait) is collected, the proposed method will classify it to gait g^*, based on the nearest multi-linear subspace criterion

$$g^* = \underset{g=1,2,3}{\text{argmax}} \left\|\mathbf{u}_g^\top \mathbf{X} \mathbf{V}_g\right\|_F^2. \tag{5}$$

That is, the classifier assigns $\mathbf{X}$ to the gait class whose TUCKER2 bases best described $\mathbf{X}$. It is interesting to notice that if $L = 1$, the 2D gait measurements become vectors and the above presented procedure simplifies to standard nearest subspace classification (NSC) [44].

IV. Experimentation

Following the data acquisition procedure presented above, we collected $N = 105$ (35 from each participant) cycles for walking, jogging, and running. After smoothing with MAF ($B = 5$), signal segmentation, and length-normalization, we obtained acceleration signatures of length $L = 283$, for each participant, gait, and axis. $N_{\text{tr}} = 90$ cycles from each gait were used for training; the remaining 15 cycles from each gait were used for testing. In Fig. 4, we plot the recognition accuracy rate of the proposed method, versus $d_{\text{time}} = 2, 3, \ldots, 6$, calculated over 2000 independent selections of training and testing data,

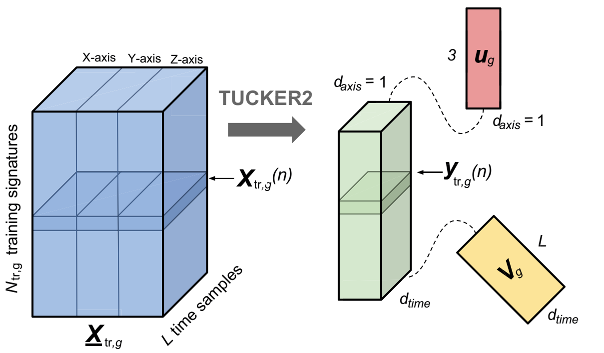

Fig. 3: Tensor structure and TUCKER2 decomposition.

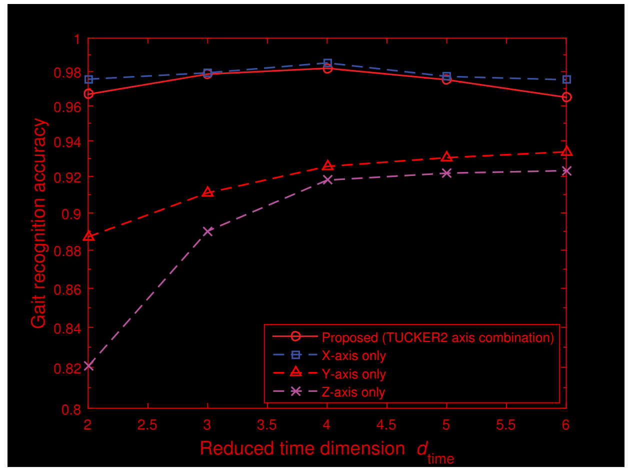

Fig. 4: Classification accuracy vs. d_{time}, for $N_{\text{tr}} = 90$.

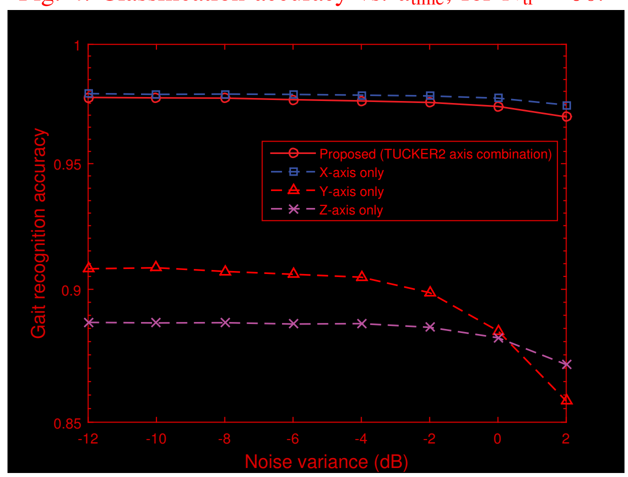

Fig. 5: Classification accuracy vs. $\sigma^2 = -12, -10, \ldots, 2$dB, for $N_{\text{tr}} = 90$ and $d_{\text{time}} = 4$.

following the standard cross-validation approach. We notice that for d_{time} as low as 4, the proposed method attains classification accuracy above 98%. Together with the proposed method, we also plot the performance of 3 alternatives: NSC only on the X-axis (equivalent to the proposed method for fixing $\mathbf{u}_g = [1, 0, 0]^\top$ for every g), NSC on the Y-axis data (i.e., $\mathbf{u}_g = [0, 1, 0]^\top$ for every g), and NSC on the Z-axis data (i.e., $\mathbf{u}_g = [0, 0, 1]^\top$ for every g). We observe that the NSC on the X-axis attains high performance, similar to that of the proposed method, while all other single-axis approaches exhibit markedly lower performance. At this point it is worth noting that in our dataset, X-axis appears to be the most discriminative axis across the three gaits (see Fig. 2). If that was known beforehand, then one could indeed operate solely on X-axis measurements and attain the high performance of Fig. 4. However, in general, such information cannot be considered available. Moreover, for more complicated gaits –not studied in this work– it is reasonable to assume that measurements from a single axis would not suffice. Quite interestingly, the proposed tensor-decomposition method was able to unveil this particular data structure in an automated way (through joint optimization in the time and axis domains), ultimately placing its focus on the X-axis. In future work, we plan to investigate classification of more complex gaits such as side-running and abnormal walking.

Next, we experiment with adding to each acceleration measurement white Gaussian noise (WGN) of variance σ^2. In Fig. 5, we fix d_{axis} to 1 and d_{time} to just 4 and plot the gait recognition accuracy of the proposed method versus noise variance $\sigma^2 = -12, -10, \ldots, 2$dB. We notice that the proposed method and the oracle-informed X-axis NSC attain classification accuracy close to 98%, superior to that of the other approaches.

V. Conclusions

We used wearable commercial sensors to collect 3D acceleration signals from walking, jogging, and running gaits. Then, we smoothed, segmented, and length-normalized the collected measurements, which we finally organized in 3-way gait tensors. Accordingly, we proposed a gait recognition method based on TUCKER2 tensor decomposition and a nearest multilinear subspace classifier. Our experimental studies showed that the proposed simple tensor-based method manages to recognize the walking, jogging, and running gaits with high accuracy.

References

1 C. Zhang, W. Liu, H. Ma, and H. Fu, "Siamese neural network based gait recognition for human identification," in *Proc. IEEE Int. Conf. Acoust., Speech, Signal Process.*, Shanghai, China, Mar. 2016, pp. 2832–2836.

2 N. V. Boulgouris, D. Hatzinakos, and K. N. Plataniotis, "Gait recognition: a challenging signal processing technology for biometric identification," *IEEE Signal Process. Mag.*, vol. 22, no. 6, pp. 78–90, Dec. 2005.

3 D. R. Howell, M. Beasley, L. Vopat, and W. P. Meehan III, "The effect of prior concussion history on dual-task gait following a concussion," *J. Neurotrauma*, vol. 34, no. 4, pp. 838–844, Sep. 2017.

4 P. Terrier, J. Le Carré, M.-L. Connaissa, B. Léger, and F. Luthi, "Monitoring of gait quality in patients with chronic pain of lower limbs," *IEEE Trans. Neural Syst. Rehab. Eng.*, vol. 25, no. 10, pp. 1843–1852, Mar. 2017.

5 J. Pärkkä, S. Mahdiani, M. Bruun, M. Baroni, H. Rhodius-Meester, S.-K. Herukka, M. van Gils, S. Hasselbalch, P. Mecocci, W. van der Flier, A. Remes, H. Soininen, and J. Lötjönen, "Gait as predictor of dementia," in *Proc. 27th Alzheimer Europe Conf.*, Berlin, Germany, Oct. 2017.

6 J. Klucken, J. Barth, P. Kugler, J. Schlachetzki, T. Henze, F. Marxreiter, Z. Kohl, R. Steidl, J. Hornegger, B. M. Eskofier, and J. Winkler, "Unbiased and mobile gait analysis detects motor impairment in Parkinson's disease," *PloS One*, vol. 8, no. 2, pp. e56 956:1–9, Feb. 2013.

7 A. Muro-de-la Herran, B. Garcia-Zapirain, and A. Mendez-Zorrilla, "Gait analysis methods: An overview of wearable and non-wearable systems, highlighting clinical applications," *Advances in Pediatrics*, vol. 14, no. 2, pp. 3362–3394, Feb. 2014.
8 A. Mannini, D. Trojaniello, A. Cereatti, and A. M. Sabatini, "A machine learning framework for gait classification using inertial sensors: Application to elderly, post-stroke and huntingtons disease patients," *Sensors*, vol. 16, no. 1, pp. 134:1–14, Jan. 2016.
9 D. Jarchi, J. Pope, T. K. Lee, L. Tamjidi, A. Mirzaei, and S. Sanei, "A review on accelerometry based gait analysis and emerging clinical applications," *IEEE Rev. Biomed. Eng.*, Feb. 2018.
10 M. G. Amin, F. Ahmad, Y. D. Zhang, and B. Boashash, "Micro-doppler characteristics of elderly gait patterns with walking aids," in *Proc. SPIE Radar Sensor Tech. XIX; Act. Pass. Sign. VI*, vol. 9461, Baltimore, MD, Apr. 2015, pp. 94 611A1:1–6.
11 A. K. Seifert, A. M. Zoubir, and M. G. Amin, "Radar classification of human gait abnormality based on sum-of-harmonics analysis," in *Proc. IEEE Radar Conf.*, Oklahoma City, OK, Apr. 2018, pp. 940–945.
12 P. Lei, Y. Zhang, J. Wang, and J. Sun, "Estimation of human gait cycle based on cepstrum of radar micro-doppler signatures," in *Proc. Progress Electromag. Research Symp.*, Singapore, Singapore, Nov. 2017, pp. 2356–2359.
13 A.-K. Seifert, M. G. Amin, and A. M. Zoubir, "Toward unobtrusive in-home gait analysis based on radar micro-doppler signatures," *arXiv preprint arXiv:1809.06653*, 2018.
14 T. Wolf, M. Babaee, and G. Rigoll, "Multi-view gait recognition using 3D convolutional neural networks," in *Proc. IEEE Int. Conf. Image Process.*, Phoenix, AZ, Sep. 2016, pp. 4165–4169.
15 T. K. Lee, M. Belkhatir, and S. Sanei, "A comprehensive review of past and present vision-based techniques for gait recognition," *Multimedia Tools Appl.*, vol. 72, no. 3, pp. 2833–2869, Oct. 2014.
16 S. Sprager and M. B. Juric, "Inertial sensor-based gait recognition: A review," *Sensors*, vol. 15, no. 9, pp. 22 089–22 127, Sep. 2015.
17 C.-C. Yang and Y.-L. Hsu, "A review of accelerometry-based wearable motion detectors for physical activity monitoring," *Sensors*, vol. 10, no. 8, pp. 7772–7788, Aug. 2010.
18 A. Millecamps, K. A. Lowry, J. S. Brach, S. Perera, M. S. Redfern, and E. Sejdić, "Understanding the effects of pre-processing on extracted signal features from gait accelerometry signals," *Comput. Bio. Med.*, vol. 62, pp. 164–174, Jul. 2015.
19 E. Sejdić, K. A. Lowry, J. Bellanca, M. S. Redfern, and J. S. Brach, "A comprehensive assessment of gait accelerometry signals in time, frequency and time-frequency domains," *IEEE Trans. Neural Syst. Rehab. Eng.*, vol. 22, no. 3, p. 603, May 2014.
20 E. Sejdić, K. A. Lowry, J. Bellanca, S. Perera, M. S. Redfern, and J. S. Brach, "Extraction of stride events from gait accelerometry during treadmill walking," *IEEE J. Translational Eng. Health Med.*, vol. 4, pp. 1–11, Dec. 2016.
21 C. Wan, L. Wang, and V. V. Phoha, "A survey on gait recognition," *ACM Comput. Surveys*, vol. 51, no. 5, p. 89, Oct. 2018.
22 W. Wang, A. X. Liu, and M. Shahzad, "Gait recognition using wifi signals," in *Proc. ACM Int. Joint Conf. Perv. Ubiq. Comput.*, Heidelberg, Germany, Sep. 2016, pp. 363–373.
23 D. Kastaniotis, I. Theodorakopoulos, C. Theoharatos, G. Economou, and S. Fotopoulos, "A framework for gait-based recognition using Kinect," *Patt. Recogn. Lett.*, vol. 68, pp. 327–335, Dec. 2015.
24 S. Bei, Z. Zhen, Z. Xing, L. Taocheng, and L. Qin, "Movement disorder detection via adaptively fused gait analysis based on Kinect sensors," *IEEE Sens. J.*, vol. 18, pp. 7305–7314, May 2018.
25 A. H. Johnston and G. M. Weiss, "Smartwatch-based biometric gait recognition," in *Proc. IEEE Int. Conf. Biometrics Theory, Appl. Syst.*, Arlington, VA, Sep. 2015, pp. 1–6.
26 M. Muaaz and R. Mayrhofer, "Smartphone-based gait recognition: from authentication to imitation," *IEEE Trans. Mobile Comput.*, vol. 16, no. 11, pp. 3209–3221, Mar. 2017.
27 E. Sejdić, A. Millecamps, J. Teoli, M. Rothfuss, N. G. Franconi, S. Perera, A. Jones, J. S. Brach, and M. H. Mickle, "Assessing interactions among multiple physiological systems during walking outside a laboratory: an android based gait monitor," *Comput. Meth. Prog. Biomed*, vol. 122, no. 3, pp. 450–461, Dec. 2015.
28 R. T. Li, S. R. Kling, M. J. Salata, S. A. Cupp, J. Sheehan, and J. E. Voos, "Wearable performance devices in sports medicine," *Sports Health*, vol. 8, no. 1, pp. 74–78, Feb. 2016.
29 P. Düking, A. Hotho, H.-C. Holmberg, F. K. Fuss, and B. Sperlich, "Comparison of non-invasive individual monitoring of the training and health of athletes with commercially available wearable technologies," *Frontiers Physiology*, vol. 7, p. 71, Mar. 2016.
30 G. Lammel, "The future of mems sensors in our connected world," in *IEEE Int. Conf. Micro Electro Mechanical Systems*, Estoril, Portugal, Jan. 2015, pp. 61–64.
31 J. Han, H. S. Jeon, B. S. Jeon, and K. S. Park, "Gait detection from three dimensional acceleration signals of ankles for the patients with Parkinsons disease," in *Proc. IEEE Int. Special Topic Conf. Info. Tech. App. Biomed.*, Ioannina, Greece, 2006, pp. 1–4.
32 F. Khoshnoud and C. W. de Silva, "Recent advances in mems sensor technology–biomedical applications," *IEEE Instr. Measurement Mag.*, vol. 15, no. 1, pp. 8–14, Feb. 2012.
33 D. K. Shaeffer, "Mems inertial sensors: A tutorial overview," *IEEE Comm. Mag.*, vol. 51, no. 4, pp. 100–109, Apr. 2013.
34 G. Ciuti, L. Ricotti, A. Menciassi, and P. Dario, "Mems sensor technologies for human centred applications in healthcare, physical activities, safety and environmental sensing: a review on research activities in italy," *Sensors*, vol. 15, no. 3, pp. 6441–6468, Mar. 2015.
35 P. Pierleoni, A. Belli, L. Palma, M. Pellegrini, L. Pernini, and S. Valenti, "A high reliability wearable device for elderly fall detection," *IEEE Sensors J.*, vol. 15, no. 8, pp. 4544–4553, Aug. 2015.
36 H. Ahmed and M. Tahir, "Improving the accuracy of human body orientation estimation with wearable imu sensors," *IEEE Trans. Instr. Measurement*, vol. 66, no. 3, pp. 535–542, Mar. 2017.
37 T. G. Kolda and B. W. Bader, "Tensor decompositions and applications," *SIAM rev.*, vol. 51, pp. 455–500, Aug. 2009.
38 mbientlab. (2018) Metamotionr board. [Online]. Available: https://mbientlab.com/product/metamotionr/
39 B. Sensortec. (2018) Bmi160 imu. [Online]. Available: https://www.bosch-sensortec.com/bst/products/all_products/bmi160
40 J. Rueterbories, E. G. Spaich, B. Larsen, and O. K. Andersen, "Methods for gait event detection and analysis in ambulatory systems," *Med. Eng. & Physics*, vol. 32, no. 6, pp. 545–552, Jul. 2010.
41 B. Mariani, H. Rouhani, X. Crevoisier, and K. Aminian, "Quantitative estimation of foot-flat and stance phase of gait using foot-worn inertial sensors," *Gait & Posture*, vol. 37, no. 2, pp. 229–234, Feb. 2013.
42 P. P. Markopoulos, D. G. Chachlakis, and E. E. Papalexakis, "The exact solution to rank-1 L1-norm Tucker2 decomposition," *IEEE Signal Proc. Lett.*, vol. 25, pp. 511–515, Apr. 2018.
43 D. G. Chachlakis and P. P. Markopoulos, "Novel algorithms for exact and efficient L1-norm-based tucker2 decomposition," in *Proc. IEEE Int. Conf. Acoust., Speech, Signal Process.*, Calgary, Canada, Apr. 2018, pp. 6294–6298.
44 Y. Liu, S. S. Ge, C. Li, and Z. You, "k-ns: A classifier by the distance to the nearest subspace," *IEEE Trans. Neural Net.*, vol. 22, no. 8, pp. 1256–1268, Jun. 2011.
45 H. Lu, K. N. Plataniotis, and A. N. Venetsanopoulos, "A survey of multilinear subspace learning for tensor data," *Pattern Recognition*, vol. 44, no. 7, pp. 1540–1551, Jul. 2011.
46 H. Lu, K. N. Plataniotis, and A. N. Venetsanopoulos, "MPCA: Multilinear principal component analysis of tensor objects," *IEEE transactions on Neural Networks*, vol. 19, no. 1, pp. 18–39, 2008.
47 W. Gong, M. Sapienza, and F. Cuzzolin, "Fisher tensor decomposition for unconstrained gait recognition," *Training*, vol. 2, no. 3, 2013.
48 H. Lu, K. N. Plataniotis, and A. N. Venetsanopoulos, "Boosting discriminant learners for gait recognition using MPCA features," *EURASIP J. Image Video Process.*, no. 1, pp. 713 183:1–11, Oct. 2009.
49 X. Ben, P. Zhang, R. Yan, M. Yang, and G. Ge, "Gait recognition and micro-expression recognition based on maximum margin projection with tensor representation," *Neural Comput. App.*, vol. 27, no. 8, pp. 2629–2646, Nov. 2016.
50 B. N. Sheehan and Y. Saad, "Higher order orthogonal iteration of tensors (HOOI) and its relation to PCA and GLRAM," in *Proc. SIAM Int. Conf. Data Mining*, Minneapolis, MN, Apr. 2007, pp. 355–365.
51 L. Zhan *et al.*, "Multiple stages classification of Alzheimers disease based on structural brain networks using generalized low rank approximations (GLRAM)," *Computational Diffusion MRI*, vol. 39, pp. 35–44, Sep. 2014.